HYDROTHERMAL SYNTHESIS OF ZEOLITES FROM COAL FLY ASH

O.B. Kotova[1], I.N. Shabalin[2], D.A. Shushkov[1], L.S. Kocheva[1]

[1]IG KomiSC of UB of RAS, Russia, kotova@geo.komisc.ru

[2]The University of Salford, United Kingdom, i.shabalin@salford.ac.uk

Abstract.

The fly ash, from the combustion of coal to produce energy and heat, is industrial waste, which large accumulations represent a serious environmental threat. To reduce the environmental burden and improve the economic benefits of energy production the science and industry focus on the transformation of coal combustion by-products into new functional materials. The fly ash was studied by modern analytical methods. As a result of the hydrothermal reaction several types of zeolites were synthesized from the fly ash: analcime, faujasite (zeolite X) and gismondine (zeolite P). It was shown that the experimental conditions (temperature, reaction time and alkali concentration) have a significant influence on the type of zeolite and its content in the reaction products. The series of experiments resulted in building approximate crystallization field of zeolites and other phases as the first stage of the formation of ceramic membrane and other materials.

Keywords: zeolites, coal fly ash, hydrothermal synthesis, sorbents

Introduction

Fly ash is bulk industrial waste of coal combustion in thermal power plants (TPP), steel mills, etc. Therefore the problem of utilization of this technogenic waste, occupying large areas and causing damage to the environment, is very important. Many papers were published on the properties of fly ash and possibilities of its use [1-5]. Nevertheless the development of advanced technologies for the utilization of fly ash remains an important task. One of their solutions may be represented by the synthesis of zeolites from fly ash. Conversion of the fly ash in zeolites has many applications, including ion exchange, molecular sieves and adsorbents [6-8]. Identification of new applications has a real commercial interest: the list of marketable products is expanding and energy costs are reduced, environmental risks are reduced, the efficiency of sustainable development in the region is increased. Coal fly ash contains significant amounts of SiO_2, Al_2O_3 and other oxides, which are regarded as cheap raw for the ceramic industry. Technologies of zeolite synthesis from fly ash are being constantly improved in both the experimental (variations of temperature, pressure, co-reagent and other methods of exposure) sphere, and the material composition of the initial raw [9-11]; the quality, function and cost of final product depend on it.

The synthesis of zeolites from fly ash is the first stage in the formation of ceramic materials (ceramic membranes), which defines the significance of this trend of research.

The aim of this work is to develop the scientific basis for the formation of ceramic materials with given properties, in order to achieve that it is important to determine material composition of the fly ash produced from coal combustion at thermal power stations of Pechora coal basin as raw for ceramic membranes and ceramic materials.

Objects and Methods

For the experiments we used the fly ash from thermal power plants of Pechora coal basin.

The synthesis methods of zeolites were based on [9]. Firstly, using a magnetic separator we removed ferriferous phases, which do not participate in the synthesis of zeolites. Dry fly ash is mixed with the solution of sodium hydroxide (NaOH) in a certain ratio, mixed thoroughly, and the suspension was placed in an autoclave. The resulting products of hydrothermal reaction was washed with distilled water and dried. This resulted in powders consisting of the mixture of zeolite and unreacted residue in various proportions.

The chemical composition of the fly ash and the products of hydrothermal reaction was determined as follows: Na_2O, K_2O, FeO, LOI, CO_2, obtained by the complete silica analysis, the other components - with the help of X-ray fluorescence analysis (energy dispersive spectrometer MESA500W, Horiba).

The phase composition studies were performed on powder diffractometer (Shimadzu XRD 6000, radiation CuK_α, Ni filter) within range 2 - 65° 2θ angle with rate 2° 2θ/min. Identification of zeolites was carried out using databases «WWW-MINCRYST» (http://database.iem.ac.ru/mincryst/rus/index.php) and International Zeolite Association (http://www.iza-structure.org/databases).

To study the morphology and chemical composition of the fly ash we used a scanning electron microscope TESCAN VEGA 3 LMH with energy dispersive Oxford Instruments X-Max.

Results and discussion

Initial fly ash. X-ray diffraction (Fig. 2) showed quartz, mullite, magnetite and hematite in the fly ash. The broad "hump" (area of increased background) on the diffraction pattern in the area 15–35 °2θ indicates the presence of amorphous phase (probably silicate or aluminosilicate glass).

The main components of the chemical composition are oxides of silicon (57.78 %) and aluminum (18.25%), iron oxide content is about 9.0 %, oxides of other elements - 7.42 %, LOI - 7.90 % (Table 1).

The fly ash is represented under the electron microscope by globules (Fig. 1), which are divided by the chemical composition to oxide-aluminosilicate and oxide-ferriferous. The globules composition is predominated by silica (from 41.82 to 61.27 %) and alumina (from 17.03 to 22.8 %), the oxides of iron (up to 8.31 %), magnesium (up to 4.83 %), potassium (up to 3.05 %), titanium (up to 1.04 %) and sodium (up to 0.93 %) are also present. Globule size varies from the first to about hundred micrometers; on the surface bubbles and elongated structures (Fig. 1b) are observed.

On the surface of iron oxide globules (Fig. 1 c, d) both flat areas and skeletal forms are observed, which are significantly different from each other by their chemical composition. The skeletal forms have a high content of iron oxides (68.14-74.66 %) and low silica (1.06-6.22 %), alumina (1.33-4.17%) and calcium oxide (0.48-3.59%) contents. On the flat areas iron oxide content is greatly reduced (19.29-31.81 %), silica and alumina content increases (27.12-37.86 and 2.06-6.22 % respectively); calcium is present in large amounts (10.45-25.3 %). Globule size ranges from several to tens micrometers. Globules, which contain smaller globules within, are often present (Fig. 2b).

Hydrothermal synthesis. There were two sets of experiments. In the first set the effect of temperature of hydrothermal reaction on zeolite synthesis was studied (reaction temperature 80, 95, 140 and 180 °C, reaction time 12 hours, the ratio of NaOH: fly ash = 1:1, NaOH concentration 3.0 mol/dm^3). The second set of experiments studied the influence of reaction time and concentration of alkali on synthesis process (reaction temperature 140 °C, duration 2, 4, 6 and 8 hours, ratio of NaOH: fly ash = 1:1, NaOH concentration 1.5, 3.0 and 4.5 mol/dm^3).

The process of transformation of the fly ash to zeolites can be represented in the following way:

$$\underbrace{\left(SiO_2 + 3Al_2O_3 \cdot 2SiO_2 + aluminosilicate\ glass\right)}_{\text{Fly ash (solid)}} + \underset{\substack{\text{Aqueous}\\ \text{solution}}}{NaOH} \xrightarrow{T=80\text{–}180^oC}$$

$$\xrightarrow{T=80\text{–}180^oC} \underbrace{SiO_4^{4-} + AlO_4^{5-} + Na^+ + OH^-}_{\text{Reaction mix}} \rightarrow \underset{\substack{\\ \text{Zeolite}}}{Na_{x/n}[Al_xSi_yO_{2(x+y)}]} \cdot zH_2O$$

where n in zeolite formula – oxidation degree, which is equal to 1 for Na.

According to [10, 11], this process consists of three stages: dissolution, condensation and crystallization. When fly ash interacts with sodium hydroxide it is dissolved, and Si and Al are released to the solution. Then the condensation of silicon and aluminum ions occurs, followed by gelling and nucleation (forming nuclei or crystallization centers) and crystallization of zeolites.

The synthesis results in powders consisting of the mixture of zeolite and unreacted residue in different proportions, which output was 70-80 % of the weight of the initial fly ash. The bulk density of powder is 0.78-0.83 g/cm^3.

Effect of reaction temperature on the synthesis of zeolites. In the result of the reaction at 80 °C the intense reflections of quartz were diagnosed; no newly formed phases were detected (Fig. 2). Electron microscopic studies revealed numerous globules destroyed by alkaline solution.

By increasing the reaction temperature to 95 °C silica the intensity of quartz reflections decreased, i.e. it was dissolved in alkaline solution. Alongside with quartz reflections the intense reflections were determined, which are characteristic for faujasite zeolite (zeolite A), and weak reflections characteristic for gismondine zeolites (zeolite P). By Si/Al ratio the zeolites are low silica: silica-aluminum module of zeolite X varies from 1.51 to 1.57, zeolite P - from 1.65 to 1.69. SEM images present numerous crystals of zeolite X with octahedral shape with the size of 1-3 mm (Figure 3 a, b). Zeolite P crystals have a rounded shape, their size is about 5 microns (Figure 3 b).

The diffraction patterns of the reaction products obtained at 140 °C showed zeolite P and analcime, weak quartz reflections were also present. Zeolite P is more high-silica compared to the phase obtained at 95 °C: Si/Al ratio varies slightly from 1.93 to 1.94. Silica-aluminum module of analcime varies from 2.12 to 2.21. SEM images showed that zeolite P formed skeletal crystals with size of 10-15 microns (Fig. 4 a). Analcime crystals with size of 15-20 microns were observed (Fig. 4 b).

The reaction at 180 °C resulted in the formation of analcime and cancrinite; no quartz reflections were diagnosed. Si/Al ratio of analcime varies from 2.00 to 2.15. As seen in Fig. 6a, the analcime crystals are formed by tetragonal faces, their size ranges from 15 to 25 microns. Cancrinite columnar crystals with length of up to 2 micrometers and about 200-300 nm in diameter (Fig. 5 b) are often observed on the surface of analcime, indicating later crystallization of cancrinite.

These results indicate that the reaction temperature influences the type of synthesized zeolite, which differ by the efficient diameter of entrance windows, and according to classification [12], they are divided into narrow, medium and wide porous types. It is determined that increasing reaction temperature results in the formation of narrow porous zeolites; at 95 °C zeolites X formed that are related to wide porous type, at 140 °C – zeolite P, related to medium porous type, and at 180 °C – analcime related to narrow porous zeolite.

Effect of reaction time and alkali concentration on zeolite type. The set of experiments resulted in the apporoximate crystallization field of zeolites and other phases (hydrosodalite) at 140 °C, the reaction time from 2 to 8 hours, NaOH concentration 1.5, 2.9 and 4.5.

As seen in Fig. 6 the wide porous zeolites X are formed by 4 hours of reaction at a high concentration of alkaline solution (4.5 mol/dm3). Longer reaction leads to the disappearance of the metastable phases of zeolite X and the occurrence of more thermodynamically stable - zeolite P and then analcime.

Zeolite P is crystallized under a wide range of reaction conditions. At the same time, the fields of crystallization of analcime and zeolite P are significantly overlapped, that is, at the same conditions of the hydrothermal reaction, the mixture of zeolites in various quantitative relations is formed. Higher concentrations of alkali results in the increase of the content of narrow porous phases (analcime) compared to zeolite P, and contributes to the formation of non-zeolitic phase - hydrosodalite.

Conclusions

Several types of zeolites: analcime, faujasite and gismondine zeolites were synthesized as the result of hydrothermal reaction at 80 – 180 °C from the fly ash of power plant (Pechora coal basin, Russia) by adding sodium hydroxide at concentration from 1.5 to 4.5 mol/dm^3. The final product was powder: mix of zeolite and unreacted residue in various ratios with yield 70-80 % to the weight if initial fly ash. The bulk density was 0.78-0.83 g/cm^3. We determined that the reaction temperature affects the type of synthesized zeolites: wide porous zeolites were formed at 90-100 °C, increasing reaction temperature results in the formation of medium and narrow porous types. It is shown that the type of zeolite and its content in the reaction products are significantly affected by the reaction time and the concentration of alkali. The experiments resulted in the approximate crystallization field of zeolites and other phases as the first stage of ceramic formation.

Acknowledgement

This work was supported by the Program of UB RAS (project 15-18-5-45).

References

[1] Z. T. Yao, X. S. Ji, P. K. Sarker, J. H. Tang, L. Q. Ge, M. S. Xia, Y. Q. Xi. A comprehensive review on the application of coal fly ash. Earth Science Reviews, 2015, 141: 105–121.

[2] R. S. Blisset, N. A. Rowson. A review of multi-component utilization of coal fly ash. Fuel, 2012, 97: 1–23.

[3] S. Wang, H. Wu. Environmental-benign utilization of fly ash as a low-cost adsobents. Journal of Hazardous Materials, 2006, B136: 482–501.

[4] T. Uchikoshi, L. Kreethawate, C. Matsunaga, S. Larpkiattaworn, S. Jiemsirilers, L. Besra. Fabrication of ceramic membranes on porous ceramic support by electrophoretic deposition. Advances in Applied Ceramics, 2014, 113, 1: 3–7.

[5] O. B. Kotova, I. L. Shabalin, D. A. Shushkov, A. V. Ponaryadov. Sorbents based on mineral and industrial materials for radioactive wastes immobilization. Vestnik IG Komi SC UB RAS, 2015, 2: 32–34.

[6] M. Ahmaruzzaman. A review on the utilization of fly ash. Progress in Energy and Combustion Science, 2010, 36: 327–363.

[7] X. Querol, N. Moreno, J. C. Umana, A. Alastuey, E. Hernandez, A. Lopez-Soler et al. Synthesis of Zeolites from coal fly ash: an overview. Int. J. Coal. Geol., 2002, 50: 413 – 23.

[8] C. F. Wang, J. S. Li, X. Sun, L. J. Wang, X. Y. Sun. Evaluation of Zeolites synthesized from fly ash as a potential adsorbents for wastewater containing heavy metals. J. Environ. Sci., 2009, 21, 127–136.

[9] C. Belviso, F. Cavalcante, A. Lettino, S. Fiore. Zeolite synthesis from fused coal fly ash at low temperature using seawater crystallization. Coal Combustion and Gasification Products Journal, 2009, 1: 8–13.

[10] T. Walek, F. Saito, Q. Zhang, J. Kano. Zeolite from Fly Ash: Current Processes and Their Benefits and Drawbacks. Bull. Inst. Adv. Mater. Process., Tohoku University, 2007, 63: 86–95.

[11] N. Murayama, H. Yamamoto, J. Shibata. Mechanism of zeolite synthesis from fly ash by alkali hydrothermal reaction. International Journal of Mineral Processing, 2002, 64: 1–17.

[12] N. F. Chelischev, B. G. Berenstein, V. F. Volodin Zeolites as a new type of mineral raw. Moscow, 1987: 14. (in Russian)

Figure captions and table

Fig. 1: SEM photographs of surface of aluminum silicate (a, b) and iron-containing globules (c, d).

Fig. 2: Diffraction patterns of products synthesized at 80, 95, 140 and 180 °C for 12 hours (Q - quartz, X – zeolite X, P – zeolite P, A - analcime, K - cancrinite). The interplanar distances are given in Å.

Fig. 3: SEM photographs of products synthesized at 95 °C: a - accumulation of zeolite X crystals, b - crystals of zeolites X and P.

Fig. 4: SEM photographs of products synthesized at 140 °C: a - single crystal of zeolite P, b - analcime and zeolite P crystals.

Fig. 5: SEM photographs of products synthesized at 180 °C: a - single crystal of analcime, b - accumulation of crystals of cancrinite.

Fig. 6: Approximate field of crystallization of zeolites from the fly ash with varying times and NaOH concentrations (X – zeolite X, P – zeolite P, ANA - analcime, HS – hydroxysodalite).

Table 1: Chemical composition of the fly ash.

Component	Content, %	Component	Content, %
SiO_2	57.78	CaO	1.63
TiO_2	1.04	Na_2O	0.91
Al_2O_3	18.25	K_2O	1.29
Fe_2O_3	5.95	P_2O_5	<0.1
FeO	2.70	LOI	7.90
MnO	0.03	Total	100.00
MgO	2.52	CO_2	<0.1

Non-colour figure
Click here to download Non-colour figure: Fig 1.jpg

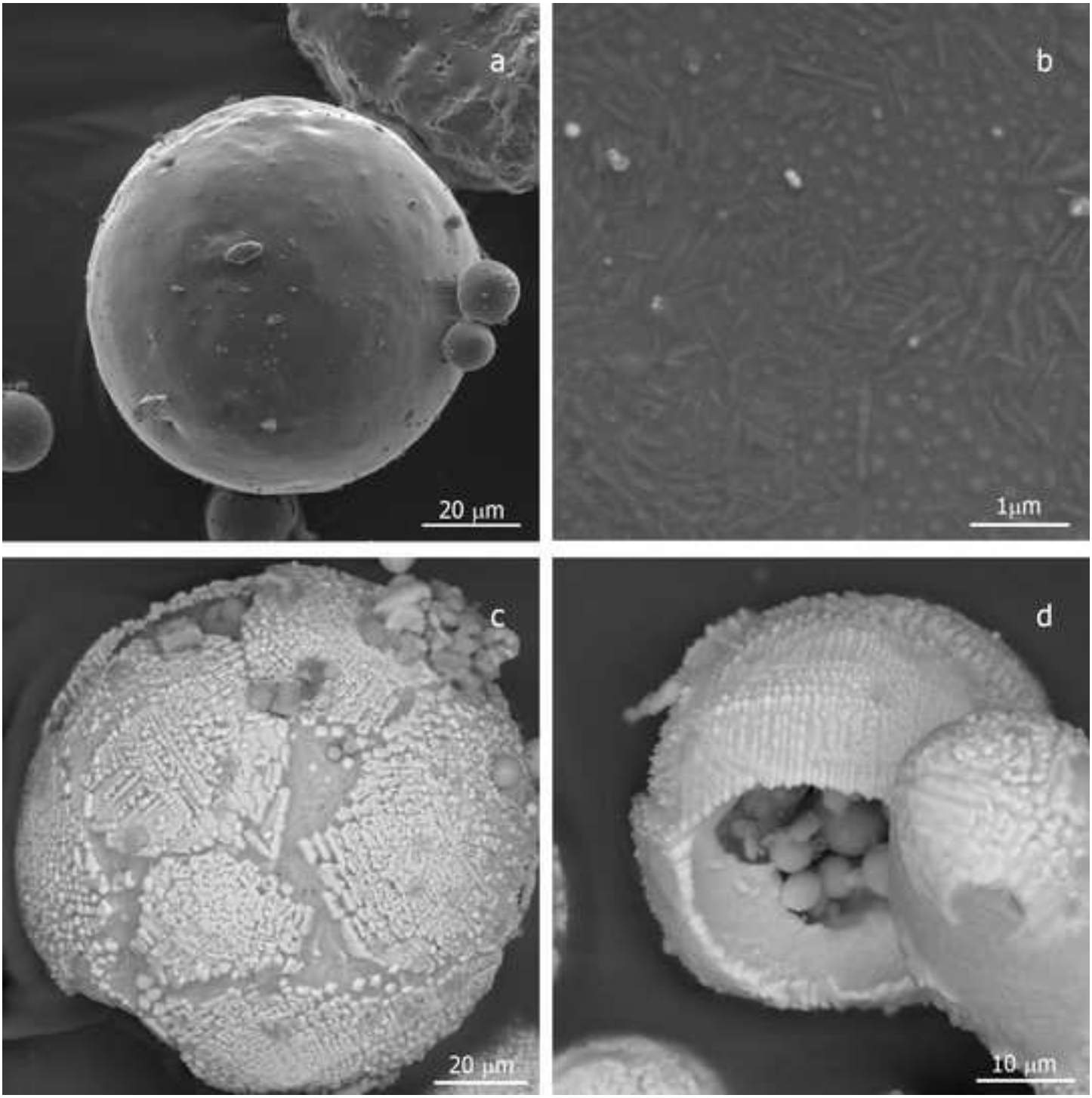

Non-colour figure

Click here to download Non-colour figure: Fig 2.jpg

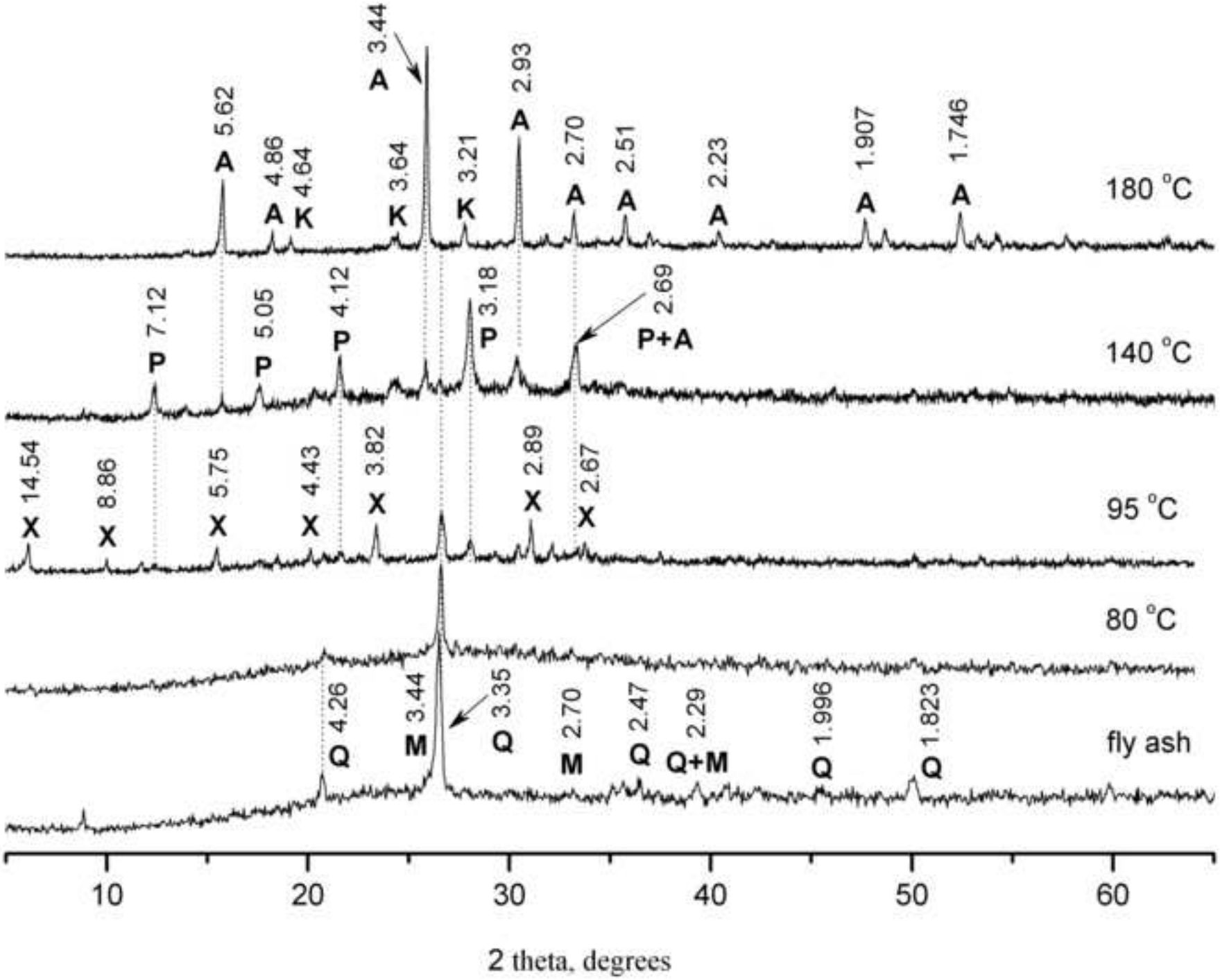

Non-colour figure
Click here to download Non-colour figure: Fig 3.jpg

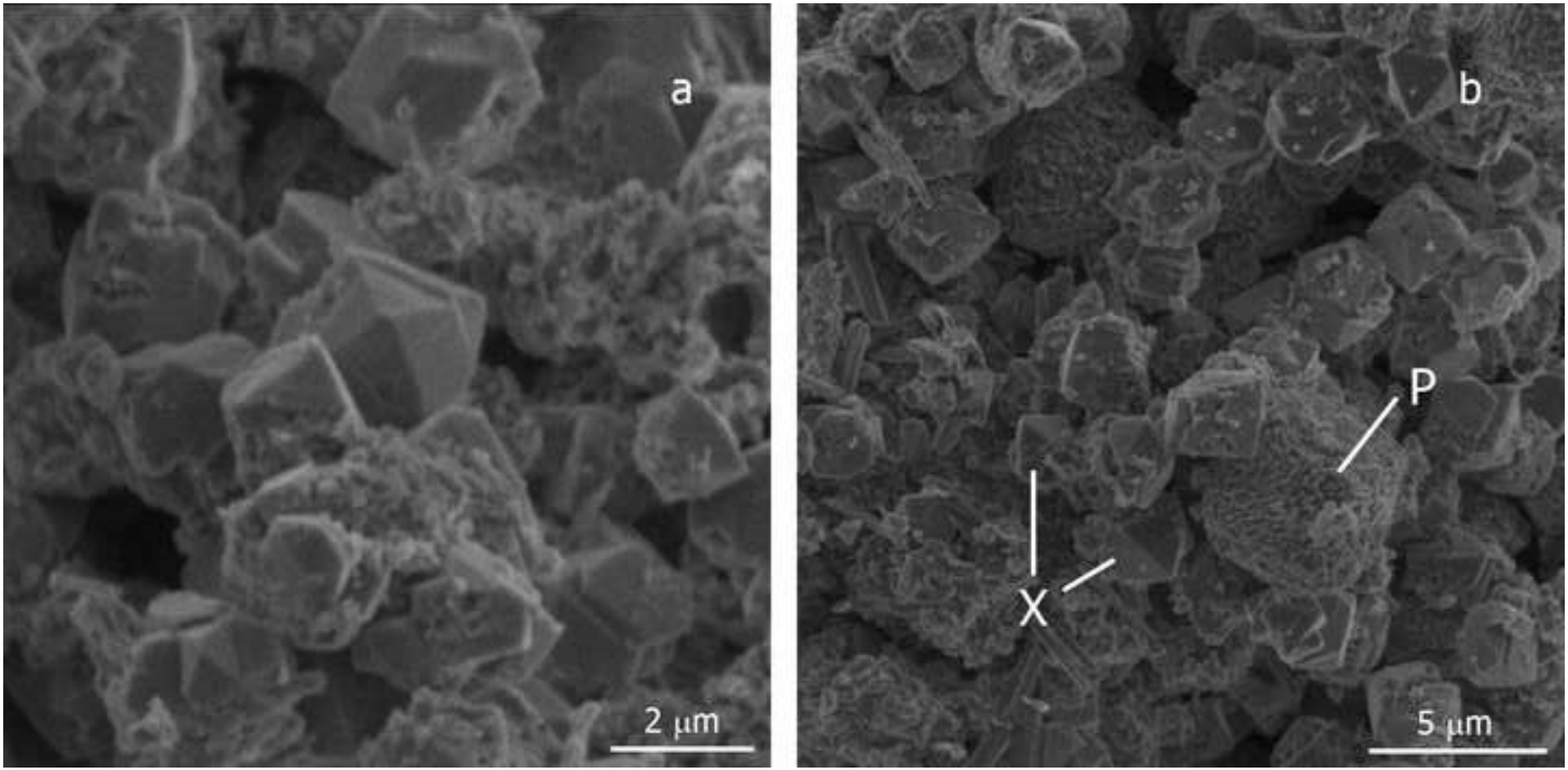

Non-colour figure
Click here to download Non-colour figure: Fig 4.jpg

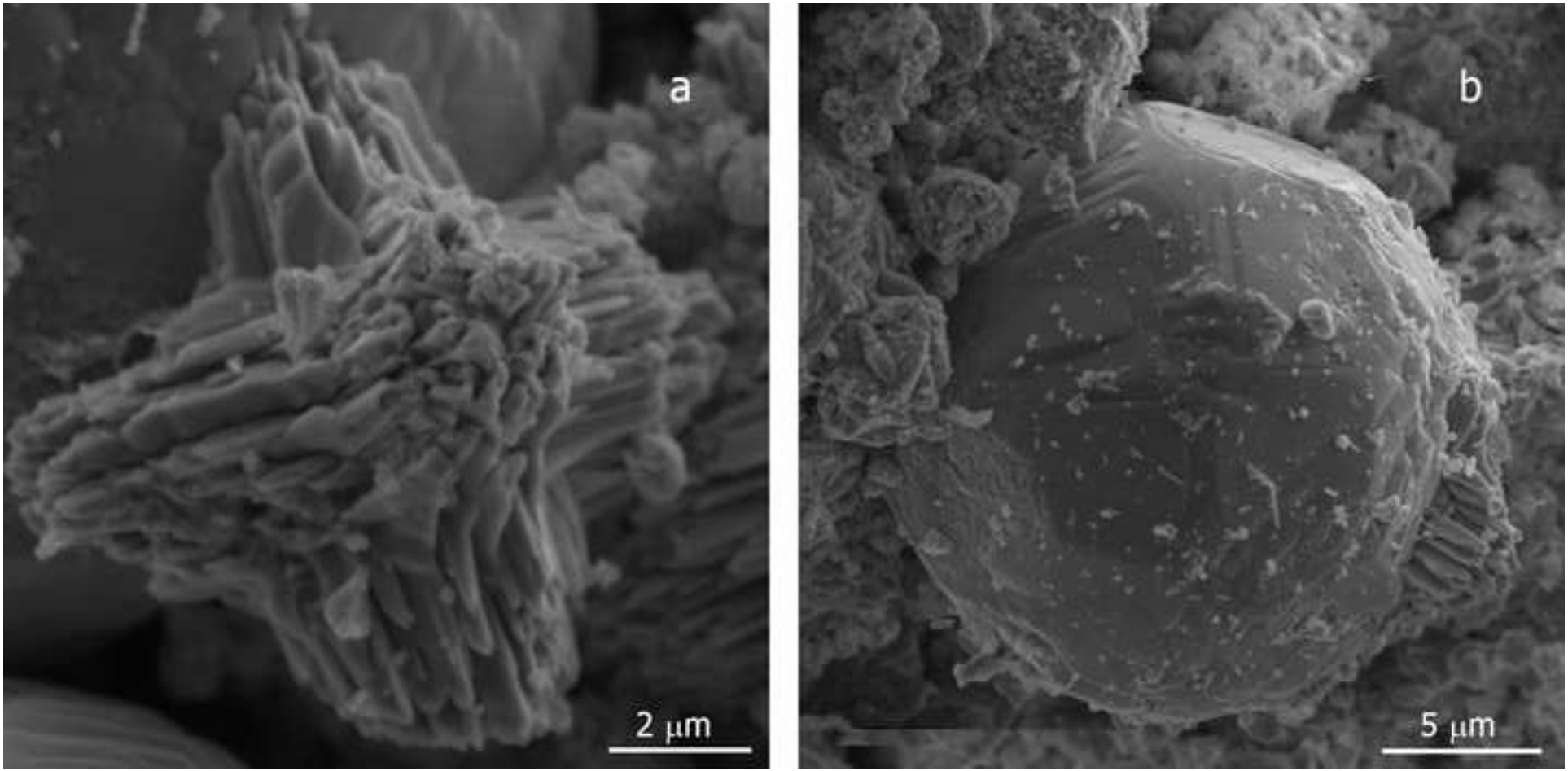

Non-colour figure
Click here to download Non-colour figure: Fig 5.jpg

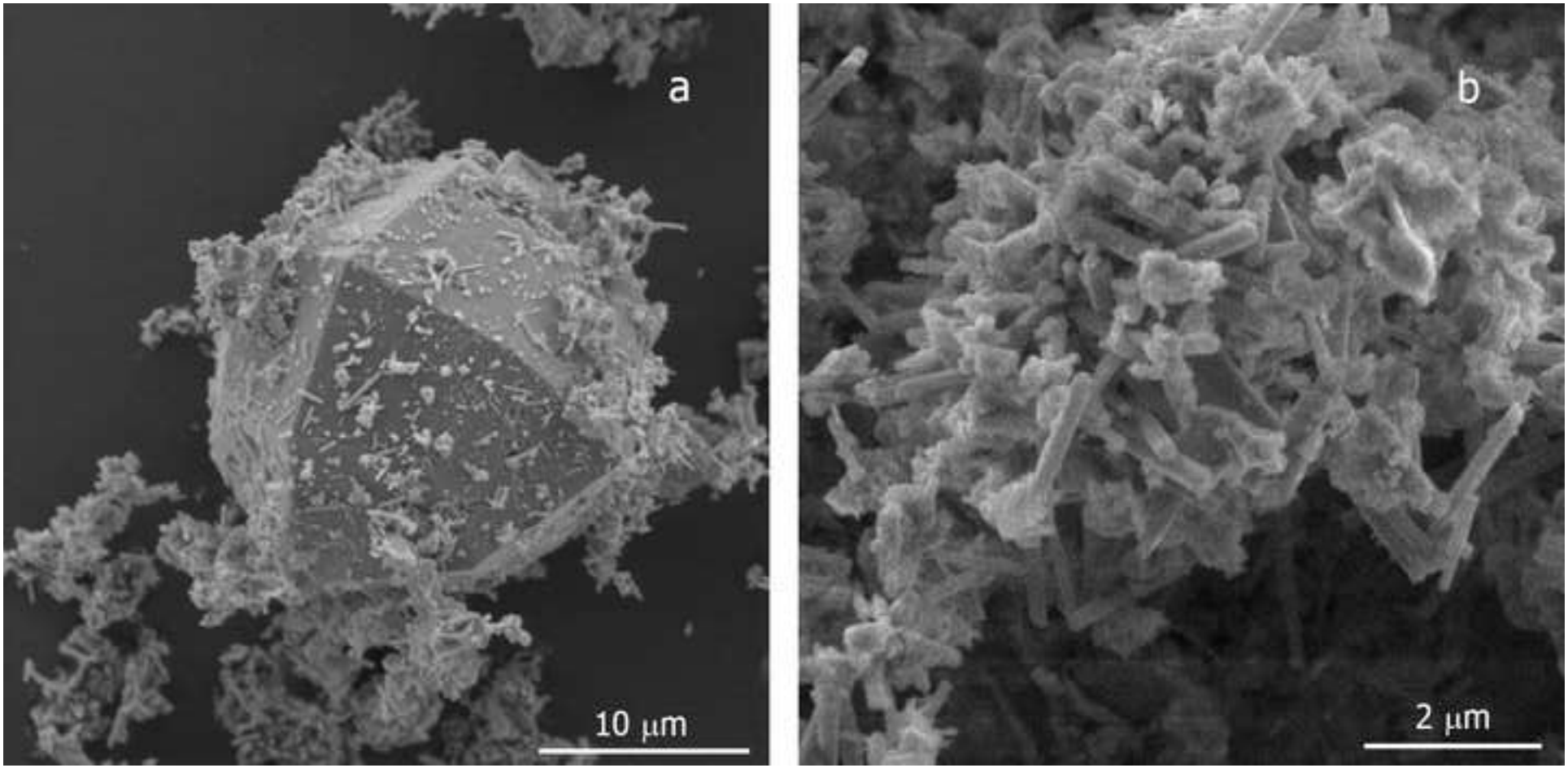

Non-colour figure
Click here to download Non-colour figure: Fig 6.jpg